

Phase diagram of thick ribbons in a bad solvent

Thanh-Son Nguyen,^{1,2} Jayanth R. Banavar,³ Amos Maritan,⁴ and Trinh X. Hoang^{1,*}

¹*Institute of Physics, Vietnam Academy of Science and Technology, 10 Dao Tan, Ba Dinh, Hanoi, Vietnam*

²*Liquid Crystal Institute, Kent State University, Kent, Ohio 44242, USA*

³*Department of Physics, University of Maryland, College Park, Maryland 20742, USA*

⁴*Dipartimento di Fisica, Università di Padova, CNISM and INFN, Via Marzolo 8, I-35131 Padova, Italy*

Ribbons are topological objects of biological and technological importance. Here, we study the folding of thick ribbons with hydrophobic surfaces in a bad solvent in regimes in which either the ribbon's thickness or the solvent molecule size is not vanishingly small compared to the ribbon's width. Extensive Monte Carlo simulations show that ribbons of various lengths and with a small stiffness adopt several distinct configurations as the ground state that include rolled (Archimedean spiral), curled, twisted and globule conformations. Analytic and numerical calculations based on the consideration of putative ground states lead to phase diagrams that qualitatively agree with the simulation results. A symmetry breaking of the planar rolled configuration in favor of the elongated twisted and the globular ribbons is observed on increasing the solvent size. Interestingly, the twisted ribbon is found as the ground state in the absence of any energetic preference for twisting. We show that the twist of the DNA double helix structure can be stabilized when modeled as a hydrophobic thick ribbon even in the limit of vanishing solvent size.

A ribbon is an intermediate object [1] between a polymer [2] and a membrane [3] and is frequently encountered in everyday life, in biology and in nanotechnology. As with a membrane, the surface of a ribbon provides a significant contact area to another surface, while its one dimensional character is useful for a variety of purposes such as taping, knotting, tying and decoration. In molecular biology, the DNA double helix structure has been seen as a twisted ribbon [4] with its sugar-phosphate backbones represented by the ribbon's edges. Notably, a certain phase difference between the two twisting edges of the ribbon is associated with the appearance of the DNA minor and major grooves [5]. In the realm of supramolecular structures, amyloid filaments [6] predominantly comprised of protein β -sheet structures [5] have the symmetry of a ribbon. Other notable examples include helical and twisted ribbons self-assembled by amphiphilic molecules [7, 8] and nanoribbons made up of a single layer of atoms, such as graphene [9].

Owing to both its 1D and 2D character, a ribbon can display distinct behaviors under various conditions [1, 10]. Gauss's *Theorema Egregium* shows that a flat ribbon can be bent into a helical (or spiral) configuration with cylindrical symmetry preserving its zero Gaussian curvature, but cannot be isometrically transformed into a twisted configuration of negative Gaussian curvature. Twisting a flat ribbon requires non-isometric deformations and may result in an increase of in-plane elastic energy [11]. There has been interest on the transition between helical and twisted ribbons [7, 8]. Selinger *et al.* have shown that such transition is smooth for ribbons formed by chiral molecules [12]. Ghafouri and Bruinsma have argued that this transition becomes discontinuous on varying the ribbon's width [11]. Hatwalne and Muthukumar have recently suggested that topological surface defects may contribute to the twisted geome-

try [13]. In these studies, chiral configurations arise from the interplay between complex elastic forces and intrinsic molecular or material properties.

In this Letter, we present a new and simple mechanism that leads to the formation of a number of characteristic conformations of a ribbon such as the rolled (Archimedean spiral [14]), the curled, the twisted and the globular conformations (Fig. 1). This mechanism does not rely on a ribbon's specific elastic properties, but rather on the geometry of the ribbon and the grained character of the surrounding solvent. In particular, we consider a hydrophobic thick ribbon in solution and study how the ribbon thickness and the solvent molecule's size may impact the ribbon's phase behavior. We will show that both the ribbon thickness and the solvent size give rise to the formation of the twisted conformation albeit the ribbon has no intrinsic elastic chiral preference. As an application, we will show how the model of hydrophobic thick ribbon can be tailored to stabilize the twist of DNA molecule.

The geometric approach employed here for the thick ribbons follows from earlier work used to model thick polymers or flexible tubes [15–18]. It has been shown that a hydrophobic tube curls into a tight helix or an almost planar sheet when immersed in water [19]. Interestingly, these emergent motifs form the building blocks of protein structures [5]. We will consider two driving forces for the folding of a ribbon: we seek to minimize the ribbon's exposed area to the solvent while minimizing its the bending energy. Based on extensive computer simulations under various conditions, we find that the ribbon commonly forms just a few optimal conformations similar to the ones shown in Fig. 1. Armed with this insight, we have carried out analytic and numerical calculations of the energies of these putative ground states and elucidate a phase diagram. These calculations are vastly

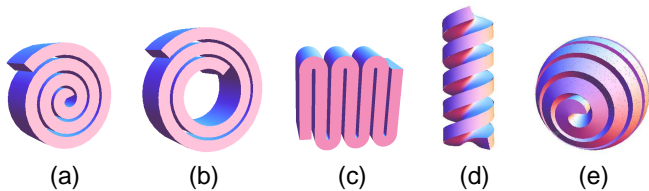


FIG. 1. Various configurations of a thick ribbon including a rolled (Archimedean spiral) conformation with no hole (a), a rolled conformation with a hole (b), a curled (c), a twisted (d) and a globular (spherical spiral) (e) conformation.

simpler than doing the simulations – ensuring that a ribbon of non-zero thickness does not self-intersect requires a set of 4-body non-local interactions [20, 21], which are highly computer intensive. As is common in such optimization problems, one cannot definitively rule out the existence of other novel ground states that we have not encountered in our simulations. However, our simulations suggest that the phase diagram we have obtained is in fact complete.

Consider a ribbon of length L , width W and thickness h . We will assume that the two main surfaces associated with the width of the ribbon (the upper and lower surfaces) are hydrophobic to the solvent, whereas the side surfaces associated with its thickness are neutral. Solvent molecules are considered as spheres of diameter D . The ribbon is considered to be flexible but its midplane surface area, width and thickness are conserved. The total energy of the ribbon (we work exclusively in the low temperature limit and do not consider entropic effects) is given by [18, 22]

$$F = \sigma S + U, \quad (1)$$

where S is the ribbon's total exposed surface area, $\sigma > 0$ is the solvent-induced energy per unit surface area, and U is the bending energy. S is defined on both upper and lower surfaces, whereas for simplicity, U is considered only for the ribbon's midplane. For the latter, we employ the Helfrich's free energy density of curvature [23]

$$f_c = \frac{\kappa}{2} H^2 + \bar{\kappa} K, \quad (2)$$

where $H = c_1 + c_2$ and $K = c_1 c_2$ are the mean and Gaussian curvatures, respectively, with c_1, c_2 the two principal curvatures of the surface [14]; κ and $\bar{\kappa}$ are bending rigidities. Note that a positive $\bar{\kappa}$ would make the twisted conformation elastically favorable because of its negative Gaussian curvature. In this study, we consider however a special case of $\bar{\kappa} = -\kappa < 0$, for which the Helfrich's free energy density reduces to a simpler form,

$$f_c = \frac{\kappa}{2} (c_1^2 + c_2^2), \quad (3)$$

with κ measured in units of σW^2 . This free energy density entails no energetic preference for both the bending

and the twisting of the ribbon. The total bending energy U is obtained by integrating f_c over the midplane. Note that the present model does not include in-plane elastic energy.

We first carried out Monte Carlo simulations of hydrophobic thick ribbons to find their ground states. A model of ribbon appropriately adapted to the general description given above is necessary for the simulations. The ribbon's midplane is represented by spherical beads on a square mesh. The beads along the ribbon's lateral dimension are always in a straight line with a fixed lattice spacing equal to b , so that the ribbon can be considered as a ladder made up of straight rungs. The bead spacing along the ribbon's central curve is also fixed and equal to b whereas on the rest of the lattice it is allowed to vary between $0.5b$ and $1.5b$ thereby permitting the ribbon to bend and twist. Self-avoidance [20, 21] requires that the radius of a sphere which is tangent to the ribbon at a given bead (in either the normal or the anti-normal direction) and passing through any of the other beads ought to be larger than $h/2$. Additionally, a hardcore radius of $b/4$ is introduced for every bead to avoid spurious overlap, given that $h > b/2$. A bending energy is applied for the beads on the central curve and is given by

$$u = \kappa_b(1 - \cos \theta) + \kappa_b(1 - \cos \phi), \quad (4)$$

where $\kappa_b = \kappa(b/W)^2$ is the stiffness per bead, the first term on the r.h.s. is the bending energy with θ denoting the bond (bending) angle at the bead and the second term is the twisting energy with ϕ representing the angle between two consecutive rungs at the given site. It is also assumed that all the beads on the same rung have the same bending energy. The ribbon exposed area is calculated by counting the number of surface elements exposed to the solvent. In order to check if an element is exposed to the solvent, one places a solvent sphere of diameter D centered at a distance of $(h + D)/2$ from a midplane bead in the normal or anti-normal direction and then checks whether it is found at a distance larger than $(h + D)/2$ from all other beads. The samplings are carried out by parallel tempering [24] simulations with pivot and reptation [2] moves.

Fig. 2 shows the ground states obtained by the simulations for ribbons of several lengths and for different solvent sizes. It is shown that for small solvent diameter ($D = 0.2W$), the ground state has a planar symmetry which can be either a curled ($L = 10W$), a rolled ($L = 30W$) or some intermediate conformation ($L = 20W$). As the solvent size increases, the planar symmetry is broken – the ground state becomes a twisted conformation for the smallest L or some sorts of globular conformation for larger L .

We have analytically and numerically determined the phase diagram of a hydrophobic thick ribbon by considering the rolled, the curled, the twisted and the globular (spherical spiral) conformations as shown in Fig. 1

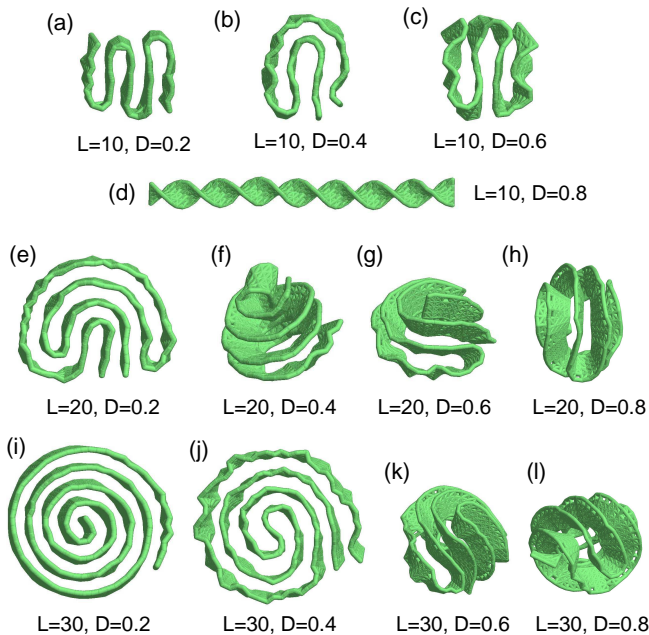


FIG. 2. Lowest energy conformations (a-l) of thick ribbons obtained by simulations for various lengths L and solvent radii D as indicated. The ribbon parameters used in the simulations are: $W = 1$ (width), $h = 0.5$ (thickness), $b = 0.2$ (bead spacing), and $\kappa_b = 0.1 \sigma b^2$ (equivalent to $\kappa = 0.1 \sigma W^2$).

as candidates for the ground state. All these conformations are parameterizable and thus their exposed area and bending energy can be precisely calculated by using differential geometry and numerical methods (see Supplemental Material [25]). For example, the midplane of the twisted ribbon is considered as an ideal helicoid [14] whose Cartesian coordinates are given by $\vec{R}_{\text{mid}}(u, z) = (u \cos kz, u \sin kz, z)$, where $u \in [-W/2, W/2]$ is the parameter of the ribbon lateral dimension and k is the wave number of the twist along the z axis. The physical surfaces of the ribbon then are constructed from the midplane. For a twisted ribbon of finite thickness h , self-avoidance imposes that $k \leq 2/h$, and thus prevents infinite twisting of the ribbon. On the other hand, the surface of a twisted ribbon is fully exposed to a solvent molecule of diameter D if

$$h + D \leq \frac{2}{k}, \quad (5)$$

otherwise it can become partially or fully buried on increasing k . An interesting property of the twisted thick ribbon, that is due to the non-zero thickness, is that the ribbon total hydrophobic surface area decreases with k . Such property is not present for the rolled and curled ribbons.

The asymptotic behaviors of the ribbon exposed area and bending energy in the putative conformations at large L can be analyzed. It is found that for compact

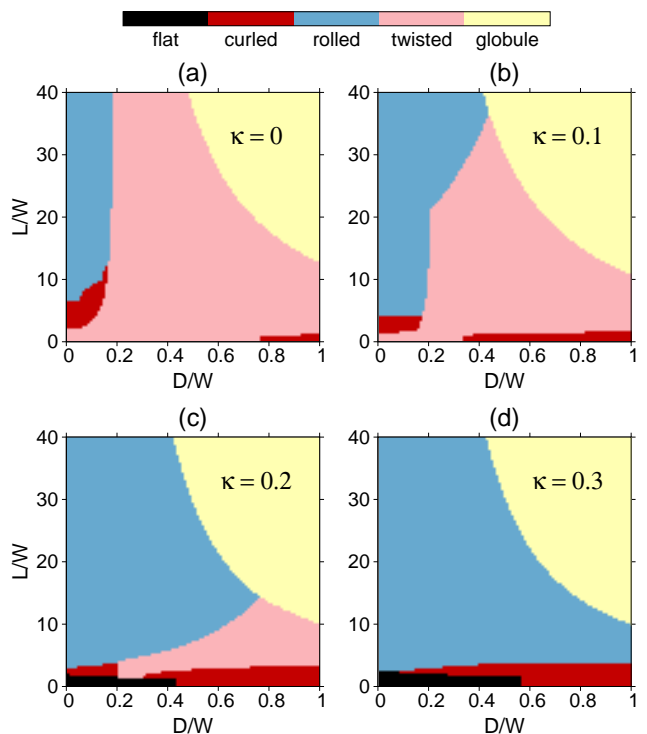


FIG. 3. Ground state phase diagram as function of the solvent diameter D and the ribbon's length L given in units of the ribbon's width W . The ribbon's thickness is $h = 0.5W$. The phase diagrams were obtained for several values of bending stiffness, $\kappa = 0$ (a), $0.1 \sigma W^2$ (b), $0.2 \sigma W^2$ (c) and $0.3 \sigma W^2$ (d). Different phases are indicated by colors as given by the legends (top).

folding

$$S_{\text{rolled}} \propto h^{1/2} L^{1/2} \quad U_{\text{rolled}} \propto h^{-1} \ln L \quad (6)$$

$$S_{\text{curled}} \propto h^{1/2} L^{1/2} \quad U_{\text{curled}} \propto h^{-3/2} L^{1/2} \quad (7)$$

$$S_{\text{twisted}} \propto L(0) \quad U_{\text{twisted}} \propto L \quad (8)$$

$$S_{\text{globule}} \propto L(0) \quad U_{\text{globule}} \propto h^{-1} \ln L, \quad (9)$$

where the subscript denotes the conformation type, and the width W of the ribbon, considered as the length unit, has been absorbed. S_{twisted} and S_{globule} are proportional to L for small D , and equal to zero for sufficiently large D . These scaling behaviors indicate that, for large L , the ground state must be either the rolled conformation or the globule because of the $\ln(L)$ dependence of their bending energy.

Fig. 3 shows the ground state phase diagram as a function of solvent diameter D and length L for a ribbon of thickness $h = 0.5W$ with several values of stiffness κ . For a given L and D , the energies of the putative ribbon conformations are minimized with respect to their geometrical parameters to identify the ground state. The curled ribbon appears as the ground state only for small L , typically smaller than $10W$. For larger L , the phase diagram is dominated either by the rolled at small D , or

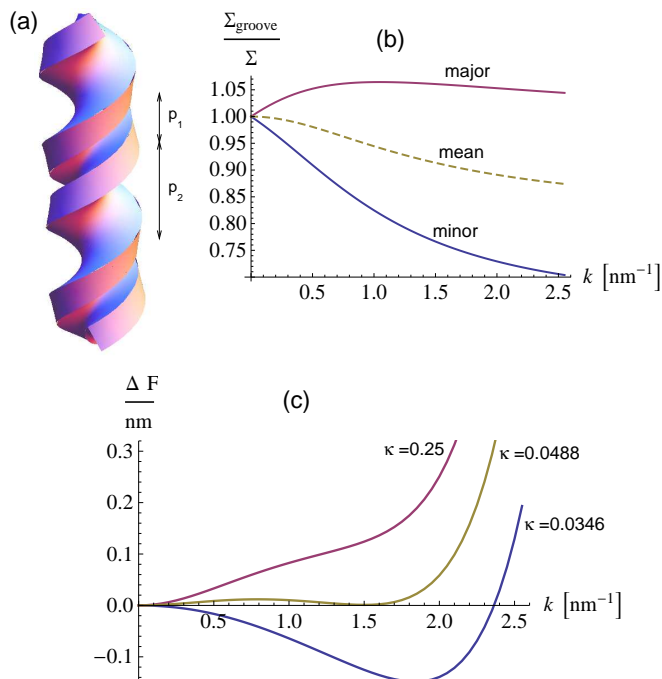


FIG. 4. (a) Thick ribbon representation of DNA molecule obtained with realistic parameters for the B-DNA double helix structure (see text). The minor and major grooves are indicated with their widths, p_1 and p_2 , respectively. (b) Dependence of the groove surface area, Σ_{groove} , relative to that of the midplane, Σ , on the wave number k of DNA twist. Dashed line corresponds to the mean area of the two grooves. (c) The energy difference ΔF per unit length between a twisted and a flat thick ribbon as a function of k , obtained with $D = 0$ for three values of κ , equal to 0.25, 0.0488 and 0.0346 σW^2 , as indicated. For the last value of κ , the minimum of ΔF corresponds to the pitch of B-DNA, $p = 3.4$ nm.

the twisted and the globular conformations at larger D . Note that the twisted phase is present only at sufficiently low stiffness, i.e. the cases of $\kappa < 0.3 \sigma W^2$ in Fig. 3. As κ increases, the twisted phase shrinks being replaced by the rolled phase and eventually disappears at high stiffness (Fig. 3d). On the other hand, for a given κ , the twisted phase also disappears on decreasing the ribbon thickness (Fig. S5, Supplemental Material).

The DNA molecule can be considered as a thick ribbon of width $W \approx 2$ nm and thickness $h \approx 0.6$ nm with the known hydrophobicity of its interstrand surfaces [5]. The DNA twist in its double helix structure, however, is not an ideal helicoid as it bends and winds differently on its two main surfaces leading to the formation of major and minor grooves. We parameterize the midplane of the DNA ribbon as

$$\vec{R}_{\text{mid}}(u, z) = (u \cos \delta \cos kz, u \cos \delta \sin kz, z + u \sin \delta), \quad (10)$$

where $u \in [-W/2, W/2]$, $k = 2\pi/p$ is the wave vector of the twist with p the helical pitch, δ is the tilt angle of the ribbon lateral direction from the plane perpendicular to

the twist axis ($\delta = 0$ for an ideal helicoid). For B-DNA, $p = 3.4$ nm is the sum of the widths, $p_1 = 1.2$ nm and $p_2 = 2.2$ nm, of the minor and major grooves, respectively (see Fig. 4a). The tilt angle can be calculated as $\sin \delta = (p_2 - p_1)/(2W)$ giving $\delta \approx 0.08\pi$. A thick ribbon presentation of the DNA twist is shown in Fig. 4a.

Our analysis shows that the DNA surface is fully accessible to a spherical molecule of diameter D if

$$h + D \leq \frac{2}{k} \frac{(1 \mp \sin \delta)}{\cos \delta}, \quad (11)$$

for the minor ($-$) and major ($+$) grooves, respectively. This gives $D \leq 0.239$ nm for the minor groove and $D \leq 0.795$ nm for the major groove. In accord with these estimates, DNA grooves are good binding sites for many ions and ligands. The groove surfaces are fully exposed to water, whose molecular diameter is about 0.14 nm. Interestingly, we find that though the groove surface area varies with k differently for different grooves, the mean surface area of the two grooves decreases with k (Fig. 4b). By using the total energy given by Eq. (1) in the limit of $D = 0$, for which the exposed area is equal to the total groove surface area, it is found that the DNA twist is stable at the experimentally observed pitch for $\kappa \approx 0.0346 \sigma W^2$ (Fig. 4c). Fig. 4c also shows that the transition from the flat phase ($k = 0$) to the twisted phase is discontinuous as the two phases are separated by an energy barrier. This symmetry breaking is due to the ribbon's non-zero thickness. We have not considered the full phase diagram for the DNA ribbon with other types of conformation. However, it can be expected that for DNA, the elongated twisted conformation is more favorable than other compact conformations, such as the rolled and the globular ones, due to strong electrostatic repulsion between DNA charges, which are presumably located on the ribbon edges.

In summary, we have shown that a simple surface energy underscoring the interaction of a ribbon with a solvent may induce dramatic changes in the ground state conformation of the ribbon, from a planar rolled conformation to the elongated twisted and the globular shapes. Such conformational changes and the associated symmetry breaking are moderated by the ribbon thickness and the solvent molecule's size. Remarkably, the phase diagram found reflects the dual characters of a ribbon, i.e. membrane-like as with the rolled conformation, and polymer-like as with the twisted and the globule conformation. Interesting, the ribbon thickness and the solvent size are shown to determine this phase behavior.

This research is funded by Vietnam National Foundation for Science and Technology Development (NAFOS-TED) under Grant No. 103.01-2016.61.

* hoang@iop.vast.vn

- [1] L. Giomi and L. Mahadevan, Phys. Rev. Lett. **104**, 238104 (2010).
- [2] P.-G. de Gennes, *Scaling Concepts in Polymer Physics* (Cornell University Press, New York, 1979).
- [3] D. R. Nelson, T. Piran, and W. Weinberg, eds., *Statistical Mechanics of Membranes and Surfaces*, 2nd ed. (World Scientific, Singapore, 2004).
- [4] A. Boudaoud, P. Patrício, and M. Ben Amar, Phys. Rev. Lett. **83**, 3836 (1999).
- [5] C. Branden and J. Tooze, *Introduction to Protein Structure* (Garland Publishing Inc., New York, 1991).
- [6] F. Chiti and C. M. Dobson, Ann. Rev. Biochem. **75**, 333 (2006).
- [7] R. Oda, I. Huc, M. Schmutz, S. J. Candau, and F. C. MacKintosh, Nature (London) **399**, 566 (1999).
- [8] L. Ziserman, A. Mor, D. Harries, and D. Danino, Phys. Rev. Lett. **106**, 238105 (2011).
- [9] A. H. Castro Neto, F. Guinea, N. M. R. Peres, K. S. Novoselov, and A. K. Geim, Rev. Mod. Phys. **81**, 109 (2009).
- [10] A. Košmrlj and D. R. Nelson, Phys. Rev. B **93**, 125431 (2016).
- [11] R. Ghafouri and R. Bruinsma, Phys. Rev. Lett. **94**, 138101 (2005).
- [12] R. L. B. Selinger, J. V. Selinger, A. P. Malanoski, and J. M. Schnur, Phys. Rev. Lett. **93**, 158103 (2004).
- [13] Y. Hatwalne and M. Muthukumar, Phys. Rev. Lett. **105**, 107801 (2010).
- [14] E. Kreyszig, *Differential geometry* (Dover Publications, New York, 1991).
- [15] A. Maritan, C. Micheletti, A. Trovato, and J. R. Banavar, Nature (London) **406**, 287 (2000).
- [16] J. R. Banavar and A. Maritan, Ann. Rev. Biophys. Biomol. Struct. **36**, 261 (2007).
- [17] Y. Snir and R. D. Kamien, Science **307**, 1067 (2005).
- [18] H. Hansen-Goos, R. Roth, K. Mecke, and S. Dietrich, Phys. Rev. Lett. **99**, 128101 (2007).
- [19] J. R. Banavar, T. X. Hoang, J. H. Maddocks, A. Maritan, C. Poletto, A. Stasiak, and A. Trovato, Proc. Natl. Acad. Sci. USA **104**, 17283 (2007).
- [20] J. R. Banavar, O. Gonzalez, J. H. Maddocks, and A. Maritan, J. Stat. Phys. **110**, 35 (2003).
- [21] T. X. Hoang, J. R. Banavar, and A. Maritan, EPL **98**, 56006 (2012).
- [22] H. Hadwiger, *Vorlesungen über inhalt, oberfläche und isoperimetrie* (Springer-Verlag, Berlin, 1957).
- [23] W. Helfrich, Z. Naturforsch C **28**, 693 (1973).
- [24] R. H. Swendsen and J.-S. Wang, Phys. Rev. Lett. **57**, 2607 (1986).
- [25] See Supplemental Material at [URL will be inserted by publisher] for the parameterizations and analyses of the ribbon's putative ground states and the DNA twist.

**SUPPLEMENTAL MATERIAL: SYMMETRY BREAKING IN THE FOLDING OF THICK RIBBONS
MODERATED BY SOLVENT**

Differential geometry of thick ribbons

Consider a ribbon of length L , width W and thickness h . Assume that the midplane of the ribbon is differentiable and in Cartesian coordinates it can be parameterized as $\vec{R}_{\text{mid}}(\alpha, \beta)$, where α and β are the parameters with $\alpha \in [\alpha_0, \alpha_m]$ and $\beta \in [\beta_0, \beta_m]$. The choice of α and β will conveniently depend on the type of ribbon conformation and will be given in the next subsections. The metric tensor [14] of the midplane can be calculated as

$$g_{\alpha\beta} = (\partial_\alpha \vec{R}_{\text{mid}}) \cdot (\partial_\beta \vec{R}_{\text{mid}}) , \quad (\text{S1})$$

where ∂_α and ∂_β are partial derivatives with respect to α and β , respectively. The determinant of this tensor is denoted as

$$g = \det(g_{\alpha\beta}) . \quad (\text{S2})$$

Assume that the surface area of the midplane is conserved and given by

$$\Sigma = \int_{\alpha_0}^{\alpha_m} d\alpha \int_{\beta_0}^{\beta_m} d\beta \sqrt{g} = LW . \quad (\text{S3})$$

The local normal vector to the ribbon midplane is given by

$$\hat{N} = \frac{(\partial_\alpha \vec{R}_{\text{mid}}) \times (\partial_\beta \vec{R}_{\text{mid}})}{|(\partial_\alpha \vec{R}_{\text{mid}}) \times (\partial_\beta \vec{R}_{\text{mid}})|} . \quad (\text{S4})$$

The ribbon physical surfaces can be constructed from the midplane as

$$\vec{R}_{\text{surface}}^\pm = \vec{R}_{\text{mid}} \pm \frac{h}{2} \hat{N} , \quad (\text{S5})$$

where \pm denote the upper and lower surfaces, respectively. One should be able to calculate the metric tensors of these surfaces

$$g_{\alpha\beta}^\pm = (\partial_\alpha \vec{R}_{\text{surface}}^\pm) \cdot (\partial_\beta \vec{R}_{\text{surface}}^\pm) , \quad (\text{S6})$$

and their determinants

$$g^\pm = \det(g_{\alpha\beta}^\pm) . \quad (\text{S7})$$

The areas of the ribbon upper and lower surfaces are then given by

$$\Sigma^\pm = \int_{\alpha_0}^{\alpha_m} d\alpha \int_{\beta_0}^{\beta_m} d\beta \sqrt{g^\pm} . \quad (\text{S8})$$

Because of the non-zero thickness, Σ^\pm are generally different from Σ . We will show later that the total surface area of a ribbon needs not to be conserved, i.e., $\Sigma^+ + \Sigma^- \neq 2\Sigma$, as found in the case of the twisted ribbon.

The surface curvatures of the midplane can be obtained by considering the second fundamental form tensor [14]

$$b_{\alpha\beta} = (\partial_{\alpha,\beta} \vec{R}_{\text{mid}}) \cdot \vec{N} . \quad (\text{S9})$$

The Gaussian curvature can be calculated as

$$K = \frac{\det(b_{\alpha\beta})}{\det(g_{\alpha\beta})} , \quad (\text{S10})$$

whereas the mean curvature is given by

$$H = \frac{1}{2} b_{\alpha\beta} g^{\beta\alpha} , \quad (\text{S11})$$

where $g^{\alpha\beta}$ is the inverse metric tensor ($g_{\alpha\gamma} g^{\gamma\beta} = \delta_\alpha^\beta$).

Exposed surface area and bending energy of the rolled (Archimedean spiral) ribbon

We consider a general case of the rolled conformation which has a hole (Fig. 1b) in the middle and whose midplane surface is parameterized as

$$\vec{R}_{\text{mid}}(\phi, z) = \left(\frac{\phi}{2\pi} p \cos \phi, \frac{\phi}{2\pi} p \sin \phi, z \right), \quad (\text{S12})$$

where $\phi \in [\phi_0, \phi_m]$ is the azimuthal angle, p is the distance between consecutive turn of the spiral, and $z \in [-W/2, W/2]$ is the ribbon's lateral coordinate. The metric tensor determinant of the midplane is obtained as

$$g = \frac{p^2(1 + \phi^2)}{4\pi^2}. \quad (\text{S13})$$

The conservation condition of the midplane surface area is given by

$$\Sigma = LW = \int_{-W/2}^{W/2} dz \int_{\phi_0}^{\phi_m} \sqrt{g} d\phi = \frac{Wp}{4\pi} \left[\phi \sqrt{1 + \phi^2} + \text{arcsinh}(\phi) \right] \Big|_{\phi_0}^{\phi_m}, \quad (\text{S14})$$

from which one can numerically calculate ϕ_m knowing ϕ_0 , L , and p . The metric tensor determinants of the ribbon's physical surfaces are given by

$$g^{\pm} = \left[\frac{p\sqrt{1 + \phi^2}}{2\pi} \pm \frac{h}{2} \left(\frac{2 + \phi^2}{1 + \phi^2} \right) \right]^2. \quad (\text{S15})$$

The surface areas of the ribbon's upper and lower surfaces can be exactly calculated as

$$\Sigma^{\pm} = \int_{-W/2}^{W/2} dz \int_{\phi_0}^{\phi_m} \sqrt{g^{\pm}} d\phi = W \left[\frac{p}{4\pi} \left(\phi \sqrt{1 + \phi^2} + \text{arcsinh}(\phi) \right) \pm \frac{h}{2} (\phi + \arctan(\phi)) \right] \Big|_{\phi_0}^{\phi_m}. \quad (\text{S16})$$

As easily seen, the total surface area of the rolled ribbon is conserved, i.e., $\Sigma^+ + \Sigma^- = 2\Sigma$.

For the self-avoidance condition, we will simply assume that $p \geq h$. For a given solvent diameter D , we will consider only the rolled conformations, such that the contact surfaces between successive turns of the roll are fully buried, which are found when $p < h + D$. In these conformations, only the outer surface and possibly also the inner surface of the spiral are exposed. The ribbon's total exposed area thus is given by

$$S_{\text{rolled}} = W \int_{\phi_m - 2\pi}^{\phi_m} \sqrt{g^+} d\phi + W \int_{\phi_0}^{\phi_0 + 2\pi} \sqrt{g^-} d\phi, \quad (\text{S17})$$

where the second term in the right hand side is included only if the hole size is larger than the solvent diameter. The integrals in Eq. (S17) are easily calculated using the result of Eq. (S16).

The Gaussian curvature of the midplane surface of the rolled conformation is always zero, while the mean curvature is obtained as

$$H = -\frac{\pi(2 + \phi^2)}{p(1 + \phi^2)^{3/2}}, \quad (\text{S18})$$

where the minus sign means that one of the principal curvatures is in opposite direction to the normal vector. For a given p , the minimum value of ϕ_0 can be obtained by requiring that the spiral radius of curvature at $\phi = \phi_0$ must be larger than $h/2$. The bending energy can be calculated as

$$\begin{aligned} U_{\text{rolled}} &= \int_{-W/2}^{W/2} dz \int_{\phi_0}^{\phi_m} \frac{\kappa}{2} H^2 \sqrt{g} d\phi \\ &= W \frac{\pi\kappa}{4p} \left[\frac{\phi(9 + 8\phi^2)}{3(1 + \phi^2)^{3/2}} + \text{arcsinh}(\phi) \right] \Big|_{\phi_0}^{\phi_m}. \end{aligned} \quad (\text{S19})$$

The optimal rolled conformation is obtained by minimizing the total energy (Eq. (1)) with respect to p and ϕ_0 . For sufficiently small stiffness, this minimization leads to a rolled conformation with no hole (Fig. 1a) with $p = h$ and $\phi_0 \approx 0.541\pi$. For $L \gg h$, one gets

$$\phi_m \approx \left(\frac{4\pi L}{h} \right)^{1/2}. \quad (\text{S20})$$

In this large L limit, the exposed area of the rolled conformation with no hole can be estimated as

$$S_{\text{rolled}} \approx 2W(\pi hL)^{1/2}, \quad (\text{S21})$$

whereas the bending energy is approximately given by

$$U_{\text{rolled}} \approx \frac{\kappa\pi W}{8h} \ln\left(\frac{16\pi L}{h}\right), \quad (\text{S22})$$

given that $\text{arcsinh}(x) = \ln(x + \sqrt{1+x^2})$.

Exposed surface area and bending energy of the curled ribbon

Suppose that the curled ribbon (Fig. 1c) has n turns. Denote r the midplane's radius of curvature at the turns. We consider only the turns with $h/2 \leq r < (h+D)/2$, so that the ribbon's inner surface associated with the turns are completely buried. By simple geometrical consideration, it can be shown that its exposed surface area for a solvent diameter D is equal to

$$S_{\text{curled}} = W \left[2 \left(\frac{L - n\pi r}{n+1} \right) + \left(r + \frac{h}{2} \right) [n\pi - 2\alpha\Theta(n-1) - 2\beta\Theta(n-2)] \right], \quad (\text{S23})$$

where $\alpha = \arcsin(\frac{D}{2r+h+D})$, $\beta = \arccos(\frac{4r}{2r+h+D})$, $\Theta(x)$ is the step function equal to 1 if $x > 0$ and 0 otherwise, n is an integer satisfying $1 \leq n \leq n_{\text{max}} \approx \frac{L}{\pi r}$. The Gaussian curvature of the midplane of the curled ribbon is always zero, while the mean curvature is non-zero only at the turns, at which $H = 1/r$. Therefore, the bending energy of the curled ribbon is given by

$$U_{\text{curled}} = \frac{\kappa n \pi W}{2r}. \quad (\text{S24})$$

The optimal curled conformation is obtained numerically by minimizing the total energy on changing r and n . Suppose that the energy minimum is observed at $r = r^*$ and $n = n^*$. The optimal conformation with $n^* = n_{\text{max}}$ may be obtained for sufficiently large solvent size ($D \gg h$) and small stiffness. In this particular conformation, denoted as 'crinkled' conformation [21], the ribbon is globally straight but locally modulated. In the limits of small solvent size ($D \ll h$) and vanishing stiffness, $n^* \approx \sqrt{n_{\text{max}} + 1} - 1$. For large length ($L \gg h$), one gets $n^* \approx (2L/\pi h)^{1/2}$ and

$$S_{\text{curled}} \approx 2W(2\pi hL)^{1/2}, \quad (\text{S25})$$

$$U_{\text{curled}} \approx \kappa W h^{-3/2} (2\pi L)^{1/2}. \quad (\text{S26})$$

Exposed surface area and bending energy of the twisted ribbon

We parameterized the midplane of the twisted ribbon (Fig. 1e) as:

$$\vec{R}_{\text{mid}}(u, z) = (u \cos kz, u \sin kz, z), \quad (\text{S27})$$

where $u \in [-\frac{W}{2}, \frac{W}{2}]$, $z \in [0, z_m]$, and k is the wave number of the twisting along the z axis. The determinant of the metric tensor of the midplane is given by

$$g = 1 + k^2 u^2. \quad (\text{S28})$$

z_m can be determined from the conservation of the midplane surface area:

$$\Sigma = LW = \int_0^{z_m} dz \int_{-W/2}^{W/2} \sqrt{g} du = z_m \left[\frac{W\sqrt{4+k^2W^2}}{4} + \frac{\text{arcsinh}(\frac{kW}{2})}{k} \right]. \quad (\text{S29})$$

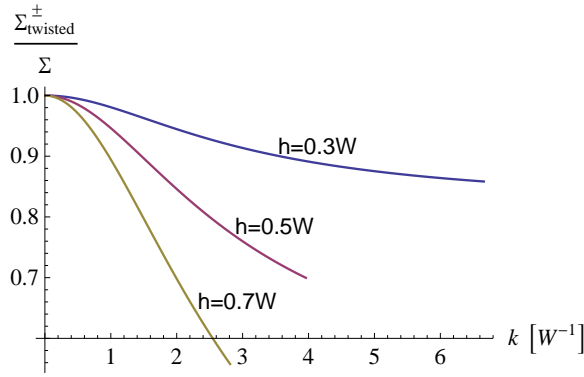


FIG. S1. Dependence of the twisted ribbon's upper and lower surface areas, $\Sigma_{\text{twisted}}^{\pm}$, on the twist's wave number k . The areas are shown relative to the midplane area Σ . The data are obtained for $h = 0.3W$, $0.5W$ and $0.7W$ as indicated. The range of k is $[0, k_{\text{max}}]$ with $k_{\text{max}} = 2/h$.

The physical surfaces of a twisted ribbon of thickness h can be constructed from the midplane using the standard procedure as given by Eq. (S5). The determinants of the metric tensors of the ribbon upper and lower surfaces are given by

$$g^{\pm} = \frac{[k^2 h^2 - 4(1 + k^2 u^2)^2]^2}{16(1 + k^2 u^2)^3}. \quad (\text{S30})$$

Note that the metric tensor determinant is the same for the upper and lower surfaces. The upper and lower surface areas of the twisted ribbon can be determined analytically and are given by

$$\Sigma_{\text{twisted}}^{\pm} = \int_0^{z_m} dz \int_{-W/2}^{W/2} \sqrt{g^{\pm}} du = z_m \left[\frac{W\sqrt{4 + k^2 W^2}}{4} + \frac{\text{arcsinh}(\frac{kW}{2})}{k} - \frac{h^2 k^2 W}{2\sqrt{4 + k^2 W^2}} \right]. \quad (\text{S31})$$

By using Eq. (S29) one obtains

$$\Sigma_{\text{twisted}}^{\pm} = \Sigma - \frac{z_m h^2 k^2 W}{2\sqrt{4 + k^2 W^2}}. \quad (\text{S32})$$

Eq. (S32) clearly shows that the surface areas of the physical surfaces of the twisted ribbon are smaller than that of the midplane and this is due to the effect of non-zero thickness h . Fig. S1 shows that the ribbon surface area decreases when either k or h increases. Note that $\Sigma_{\text{twisted}}^{\pm}$ is also the exposed area for the case of $D = 0$, thus the twisted conformation is favorable in terms of surface energy for any solvent size. We will show that this is also true for the case of DNA twist later in this supplemental material.

The ribbon thickness also has a strong effect on self-avoidance condition of the twisted conformation. If the ribbon has zero thickness, the twist's wave number k can increase to infinity while the ribbon size along the z axis shrinks to zero. If the ribbon has a finite thickness, self-avoidance prevents infinite twisting. As the wave number k increases to a certain value, the physical surface of the ribbon starts to intersect itself. The onset of self-intersection occurs exactly at the point where the metric of the surface vanishes ($g^{\pm} = 0$) and ought to happen at $u = 0$ due to symmetry. By using Eq. (S30) for g^{\pm} , one obtains the self-avoidance condition as

$$k \leq k_{\text{SA}} = \frac{2}{h}, \quad (\text{S33})$$

where k_{SA} is the self-avoidance limit of k determined by the thickness h .

For a twisted ribbon submerged in a solvent, the closest distance from the center of a solvent molecule to the ribbon midplane is $(h + D)/2$. One can construct the excluded volume surfaces as

$$\vec{R}_{\text{ES}}^{\pm} = \vec{R}_{\text{mid}} \pm \frac{h + D}{2} \hat{N}. \quad (\text{S34})$$

These new surfaces, unlike the ribbons physical surfaces, are virtual surfaces and can self-intersect. This self-intersection indicates that some regions of the ribbon physical surfaces are inaccessible to the solvent. Similarly

to the self-avoidance condition, the self-intersection happens only when k is sufficiently large, i.e.

$$k \geq k_D = \frac{2}{h+D}. \quad (\text{S35})$$

The intersection line of the excluded volume surface corresponds to the borders of the buried area on the physical surface. For the twisted ribbon, it is a helical curve lying midway between the ribbon's successive turns and has a constant u coordinate.

In order to calculate the ribbon's exposed area, we first determine the u coordinate of the excluded volume surface intersection. Thanks to symmetry, this task can be done by considering the intersection contour of one of the excluded volume surface with the $z = 0$ plane. For the upper excluded volume surface, the contour's coordinates can be found as

$$\vec{C}^+(u) \equiv \vec{R}_{ES}^+ \Big|_{z=0} = [u \cos(k^2 uv) - v \sin(k^2 uv), -v \cos(k^2 uv) - u \sin(k^2 uv), 0] \quad (\text{S36})$$

$$\text{with } v = \frac{(h+D)}{\sqrt{1+k^2 u^2}}. \quad (\text{S37})$$

The contour $\vec{C}^-(u)$ corresponding to the lower excluded volume surface can be obtained from the above equations by just changing the sign of v . Fig. S2 shows that the self-intersection of the contour occurs only on the y axis of the $z = 0$ plane. Thus, the u coordinate of the self-intersection is the solution of the following equation

$$\tan\left(\frac{k^2 u (h+D)}{2\sqrt{k^2 u^2 + 1}}\right) = \frac{2u\sqrt{k^2 u^2 + 1}}{h+D}, \quad (\text{S38})$$

which can be solved numerically. We are interested in only the solution $0 < u^* \leq \frac{W}{2}$, given that $-u^*$ is another solution by symmetry. For a given k , such that $k_D \leq k \leq k_{SA}$, and a solvent size D , solving this equation leads to one of the two following situations: (a) there is a solution $0 < u^* \leq \frac{W}{2}$ (the ribbon surfaces are partially exposed), and (b) there is no such solution (the ribbon surfaces are completely shielded). In case a, the ribbon's total exposed area on both upper and lower surfaces is given by:

$$\begin{aligned} S_{\text{twisted}} &= 4 \int_0^{z_m} dz \int_{u^*}^{\frac{W}{2}} \sqrt{g^\pm} du \\ &= 2 z_m \left(u \sqrt{1+k^2 u^2} + \frac{\text{arcsinh}(ku)}{k} - \frac{h^2 k^2 u}{2\sqrt{1+k^2 u^2}} \right) \Big|_{u^*}^{W/2}. \end{aligned} \quad (\text{S39})$$

The exposed area is equal to zero for $D > D^*$, where D^* is a solvent diameter such that $u^* = W/2$. The value of D^* can be determined numerically through Eq. (S38). It can also be shown that

$$h + D^* < \frac{\pi}{k} \sqrt{1 + (2/kW)^2}. \quad (\text{S40})$$

The midplane of the twisted conformation has a zero mean curvature, $H = 0$, as found for ideal helicoid [14]. The Gaussian curvature can be determined through calculating the second fundamental form tensor and is given by

$$K = -\frac{k^2}{(1+k^2 u^2)^2}. \quad (\text{S41})$$

The bending energy for the twisted configuration is calculated as:

$$U_{\text{twisted}} = \iint (-\kappa K) \sqrt{g} du dz \quad (\text{S42})$$

$$= \int_0^{z_m} dz \int_{-W/2}^{W/2} \frac{\kappa k^2}{(1+k^2 u^2)^{3/2}} du \quad (\text{S43})$$

$$= \kappa z_m \frac{2k^2 W}{\sqrt{4+k^2 W^2}}. \quad (\text{S44})$$

Because z_m is approximately a linear function of L , for $L \gg W$ one find that, for the twisted ribbon, $S_{\text{twisted}} \propto L$ and $U_{\text{twisted}} \propto L$.

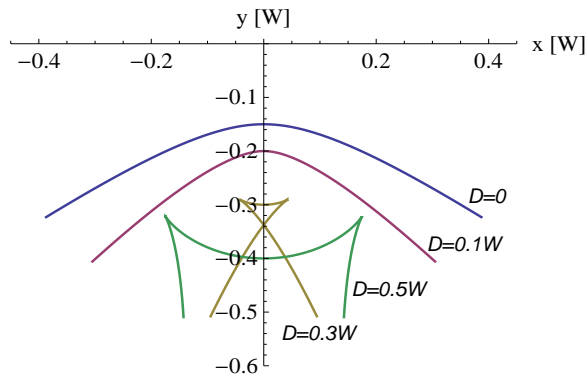


FIG. S2. Contours of the intersections of the excluded volume surface of a twisted ribbon with the $z = 0$ plane for four solvent diameters, $D = 0, 0.1W, 0.3W$ and $0.5W$, as indicated. The contours are calculated for a twisted ribbon of width $W = 1$, thickness $h = 0.3W$ and wave number $k = (4\pi/3)W^{-1}$. The self-intersection of the contour on the y axis is seen for $D = 0.3W$.

The spherical spiral (globular) ribbon

Our simulations show that for sufficiently large L and sufficiently large D , a ribbon may form compact conformations close to a globular shape with a small exposed area of its hydrophobic surface. In these globule-like conformations, the non-hydrophobic edges of the ribbon are exposed to the solvent. These conformations also display a significant helical feature. Some non-regularities observed may be due to the small sizes of the ribbons. There are many possible conformations of a globular ribbon. Here, based on the hints from simulation result, we consider a parameterized model with a globular shape, in which the ribbon forms a *spherical spiral* as shown in Fig. S3. The spherical spiral has two poles corresponding to the two ends of the ribbon. Overall, it forms a spherical layer of thickness W . The midplane of the spherical spiral ribbon can be parameterized as

$$\vec{R}_{\text{mid}}(\phi, u) = [(R + u) \sin(k\phi) \cos \phi, (R + u) \sin(k\phi) \sin \phi, (R + u) \cos(k\phi)] , \quad (\text{S45})$$

where R is the radius of the sphere passing through the central curve of the ribbon, $u \in [-W/2, W/2]$, $\phi \in [0, \phi_m]$ and $k = \pi/\phi_m$. It is straightforward to calculate the metric tensor of the midplane, whose determinant is given by

$$g = (R + u)^2 [k^2 + \sin^2(k\phi)] . \quad (\text{S46})$$

For a given ϕ_m , and $k = \pi/\phi_m$, the radius R can be determined from the midplane surface area conservation

$$\Sigma = LW = \int_{-W/2}^{W/2} du \int_0^{\phi_m} \sqrt{g} d\phi = RW \int_0^{\phi_m} \sqrt{k^2 + \sin^2(k\phi)} d\phi . \quad (\text{S47})$$

The upper and lower surfaces of the ribbon can be constructed from the midplane as shown in Fig. S3. The metric tensor determinants of these surfaces are given by

$$g^{\pm} = \left[(R + u) \sqrt{k^2 + \sin^2(k\phi)} \pm h \cos(k\phi) \frac{2k^2 + \sin^2(k\phi)}{2k^2 + 2\sin^2(k\phi)} \right]^2 . \quad (\text{S48})$$

It can be easily shown that $\Sigma^+ = \Sigma^- = \Sigma$.

To check the self-avoidance condition and to calculate the exposed area, we will employ an approximate approach by considering the cross section of the ribbon with the sphere of radius $(R + u)$. Such a cross section is a spherical spiral stripe of the width equal to

$$\mathcal{W}(u, h) = 2(R + u) \arctan \left(\frac{h}{2(R + u)} \right) , \quad (\text{S49})$$

and the midline contour length equal to

$$\mathcal{L}(u) = \int_0^{\phi_m} |\partial_{\phi} \vec{R}_{\text{mid}}| d\phi = (R + u) \int_0^{\phi_m} \sqrt{k^2 + \sin^2(k\phi)} d\phi = \frac{L(R + u)}{R} . \quad (\text{S50})$$

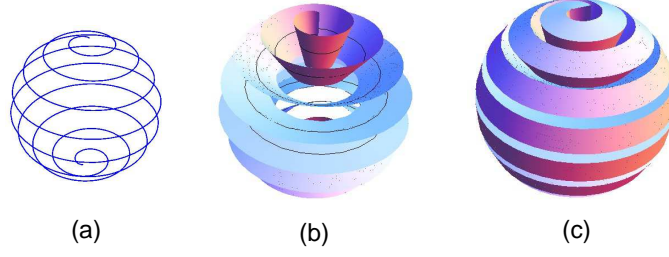


FIG. S3. (a) A spherical spiral curve. (b) The midplane of a spherical spiral ribbon with the ribbon center line following the curve shown in a. (c) A thick spherical spiral (globular) ribbon with the midplane shown in b.

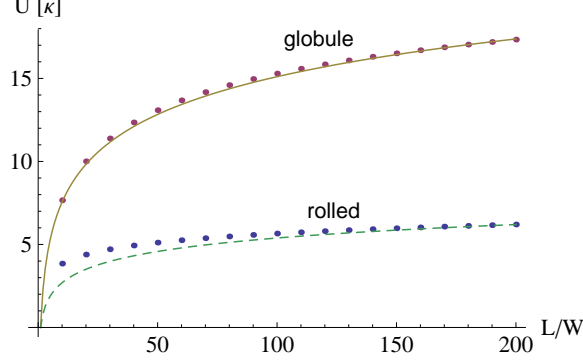


FIG. S4. Dependence of bending energy, U , on length, L , of the rolled ribbon with no hole and the spherical spiral (globular) ribbon. Discrete points are obtained by numerical evaluation, whereas smooth curves represent fits with the $\log(L)$ dependence. The data are obtained for tightly folded ribbons of thickness $h = 0.5W$.

For a self-avoiding ribbon, the area of the stripe must be not larger than the surface area of the sphere

$$\mathcal{L}(u) \cdot \mathcal{W}(u, h) \leq 4\pi(R + u)^2 \quad \Rightarrow \quad \arctan\left(\frac{h}{2(R + u)}\right) \leq \frac{2\pi R}{L}. \quad (\text{S51})$$

It is enough to check the above inequality for $u = -W/2$.

By using the same argument as above for a stripe corresponding to the excluded volume surface of the ribbon with a solvent of diameter D , one finds that the ribbon surface elements at a given parameter u is exposed to the solvent if

$$\arctan\left(\frac{h + D}{2(R + u)}\right) \leq \frac{2\pi R}{L}. \quad (\text{S52})$$

Assume that the equality of the above equation is found for u^* , such that $-\frac{W}{2} \leq u^* \leq \frac{W}{2}$, the ribbon's exposed area is given by

$$S_{\text{globule}} = 2 \int_0^{\phi_m} d\phi \int_{u^*}^{W/2} \sqrt{g^+} du = \frac{L}{R} \left(2R + \frac{W}{2} + u^*\right) \left(\frac{W}{2} - u^*\right). \quad (\text{S53})$$

By calculating the second fundamental form tensor of the midplane, one immediately finds that the spherical spiral ribbon has a zero Gaussian curvature, $K = 0$, whereas the mean curvature is given by

$$H = -\frac{\cos(k\phi)[2k^2 + \sin^2(k\phi)]}{2(R + u)[k^2 + \sin^2(k\phi)]^{3/2}}. \quad (\text{S54})$$

The bending energy thus can be numerically calculated from the integral

$$\begin{aligned} U_{\text{globule}} &= \int_0^{\phi_m} d\phi \int_{-W/2}^{W/2} du \frac{\kappa}{2} H^2 \sqrt{g} \\ &= \frac{\kappa}{8} \ln\left(\frac{2R + W}{2R - W}\right) \int_0^{\phi_m} \frac{\cos^2(k\phi)[2k^2 + \sin^2(k\phi)]^2}{[k^2 + \sin^2(k\phi)]^{5/2}} d\phi. \end{aligned} \quad (\text{S55})$$

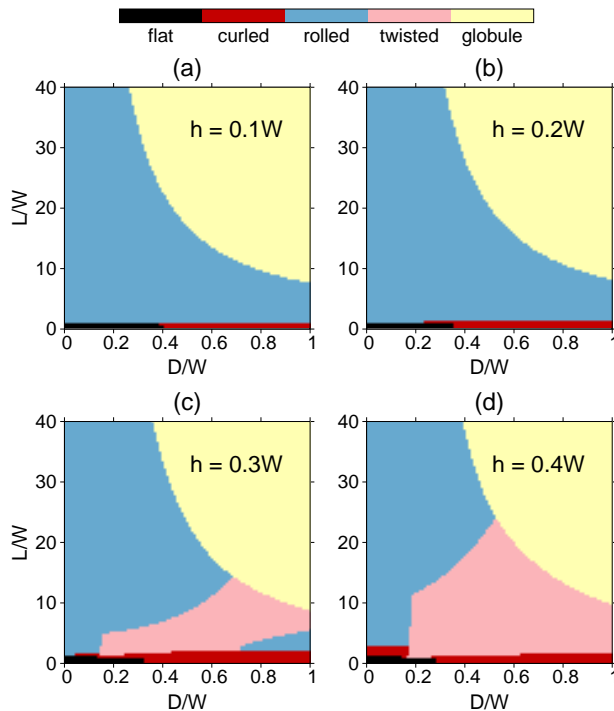


FIG. S5. Ground state phase diagram of ribbons as function of the ribbon's length L and solvent diameter D . The phase diagram is shown for different ribbon's thicknesses, $h = 0.1W$ (a), $0.2W$ (b), $0.3W$ (c) and $0.4W$ (d). The bending stiffness is $\kappa = 0.1\sigma W^2$ for all cases. Different phases are indicated by colors as given in the legends (top).

Note that R also depends on ϕ_m . Our numerical calculations indicate that the bending energy of the tightly folded spherical spiral ribbon grows logarithmically with L , similar to that of the rolled conformation (Fig. S4). It is also shown that U_{globule} is larger than U_{rolled} .

The optimal spherical spiral conformation is obtained by minimizing the total energy on changing ϕ_m . In the large length limit ($L \gg h$), one can write

$$S_{\text{globule}} \propto L \quad \text{and} \quad U_{\text{globule}} \propto \frac{W}{h} \ln L. \quad (\text{S56})$$

Ground state phase diagram of thick ribbon

We studied the ground state phase diagram of thick ribbon as function of the ribbon's length L and the solvent diameter D . For a ribbon of given L and D , together with the thickness h and stiffness κ , each of the four conformations, the rolled, the curled, the twisted and the spherical spiral ones, is optimized in terms of their total energies. The ground state is the lowest energy conformation among the four optimized configurations. Fig. 3 in the main text shows the phase diagrams for ribbons of the same thickness h but for different values of stiffness κ . On the other hand, Fig. S5 shows the phase diagrams for ribbons of the same κ but different thicknesses h . It is shown that the twisted conformation appears as the ground state for ribbons of either low stiffness (as shown in Fig. 3) or large thickness (Fig. S5).

Thick ribbon description of DNA twist

Consider the B-DNA double helix structure as a twisted thick ribbon. We parameterize the midplane of this ribbon as

$$\vec{R}_{\text{mid}}(u, z) = (u \cos \delta \cos kz, u \cos \delta \sin kz, z + u \sin \delta), \quad (\text{S57})$$

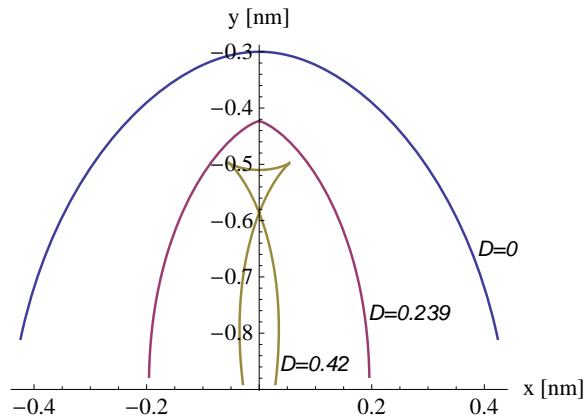


FIG. S6. Contours of the intersections of the excluded volume surface, \vec{R}_{ES}^+ , of the DNA minor groove with the $z = 0$ plane for three solvent diameters, $D = 0, 0.239$ nm and 0.42 nm, as indicated. The contours are calculated by using realistic DNA parameters of $W = 2$ nm, $h = 0.6$ nm, $p = 3.4$ nm and $\delta = 0.08\pi$. The case of $D = 0.239$ nm corresponds to the contour that is about to intersect itself at $u = 0$. For $D = 0.42$ nm, the self-intersection of the contour is seen on y axis.

where $u \in [-W/2, W/2]$ and $k = 2\pi/p$ with W and p correspond to the width and the pitch of DNA, respectively, δ is the tilt angle of the ribbon's lateral direction with respect to the plane perpendicular to the main axis of the twist (the z axis). The ribbon thickness is denoted h . One can calculate the metric tensor of the midplane and obtain the metric tensor determinant

$$g = (1 + k^2 u^2) \cos^2 \delta. \quad (\text{S58})$$

Denote h the thickness of the DNA ribbon. It is straightforward to construct the ribbon upper and lower physical surfaces $\vec{R}_{\text{surface}}^\pm$. These surfaces are shown in Fig. 4 for realistic parameters of DNA with a clear appearance of the minor (+) and major (-) grooves. The metric tensor determinants of the physical surfaces are given by

$$g^\pm = \frac{[(h^2 k^2 - 4(1 + k^2 u^2)^2) \cos \delta \pm 2hk(2 + k^2 u^2)\sqrt{1 + k^2 u^2} \sin \delta]^2}{16(1 + k^2 u^2)^3}. \quad (\text{S59})$$

Note that due to the tilt angle δ , the obtained metric tensors are different for the upper and lower surfaces. Thus, the surface areas of the grooves are also different as calculated by

$$\Sigma^\pm = \int_0^{z_m} dz \int_{-W/2}^{W/2} du \sqrt{g^\pm}. \quad (\text{S60})$$

In fact, for $k > 0$, it is found that that $\Sigma^+ < \Sigma < \Sigma^-$ and $\Sigma^+ + \Sigma^- < 2\Sigma$ with Σ the midplane area. Fig. 4b shows that the total groove surface area decreases with k .

If k is increased, the ribbon surfaces can intersect themselves. Like for the case of the ideal twisted ribbon, the self-intersection starts at $u = 0$ first with a vanishing metric at that point. The latter yields the self-avoidance condition of the ribbon as

$$h \leq \frac{2}{k} \frac{(1 \mp \sin \delta)}{\cos \delta}, \quad (\text{S61})$$

for the minor (-) and major (+) grooves, respectively. Because the minor groove yields a smaller limit for h , the self-avoidance constraint is imposed by the minor groove.

In order to calculate the exposed area of the ribbon for a solvent of diameter D , one constructs the ribbon's excluded volume surfaces \vec{R}_{ES}^\pm . The latter have the same form as $\vec{R}_{\text{surface}}^\pm$ with h being replaced by $h + D$. The ribbon surface is fully exposed to solvent if the excluded volume surface does not self-intersect, which means that

$$h + D \leq \frac{2}{k} \frac{(1 \mp \sin \delta)}{\cos \delta}, \quad (\text{S62})$$

for the minor (-) and major (+) grooves, respectively. If the excluded volume surface of a groove self-intersects, the groove surface is partially exposed. Like for the case of the ideal twisted ribbon, the u^* position of the self-intersection

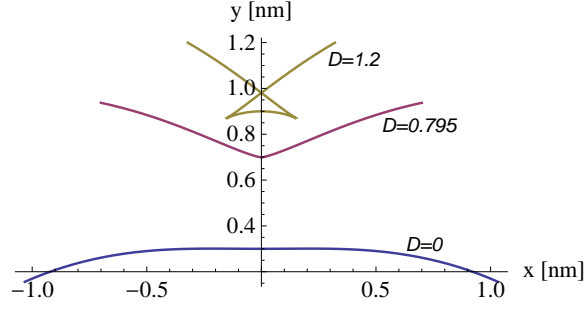


FIG. S7. Same as Fig. S6 but for the DNA major groove and for three values of solvent diameter, $D = 0, 0.795$ nm and 1.2 nm, as indicated. The case of $D = 0.759$ nm corresponds to the contour that is about to intersect itself at $u = 0$.

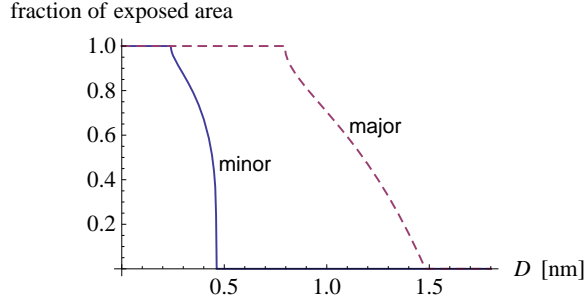


FIG. S8. Dependence of the fraction of exposed area on the solvent diameter D for the DNA minor (solid) and major (dashed) grooves. The data are obtained by using realistic parameters for DNA as given in the caption of Fig. S6.

can be determined numerically by considering the contour of the excluded volume surface \vec{R}_{ES}^{\pm} on the $z = 0$ plane. Suppose that we consider only $0 < u^* \leq W/2$. Figs. S6 & S7 show that the contour intersects itself always on the y axis and this starts happen at a lower solvent size for the minor groove. Thus, the two grooves can have different values of u^* , denoted as u_+^* and u_-^* . The exposed areas of the grooves are given by

$$S_{\text{DNA}}^{\pm} = 2 \int_0^{z_m} dz \int_{u_{\pm}^*}^{W/2} \sqrt{g^{\pm}} du . \quad (\text{S63})$$

Fig. S8 shows the dependence of the fraction of exposed area on the solvent diameter D for the two grooves.

The curvatures of the midplane of the DNA ribbon can be determined by calculating the tensors of the first and second fundamental forms. One obtains the mean curvature

$$H = \frac{k(-2 + k^2 u^2 + k^4 u^4 \cos^2 \delta) \sin(2\delta)}{4\sqrt{1 + k^2 u^2}} , \quad (\text{S64})$$

and the Gaussian curvature

$$K = -\frac{k^2}{(1 + k^2 u^2)^2} . \quad (\text{S65})$$

Note that unlike the ideal helicoid, the mean curvature of the DNA midplane is mostly non-zero for $\delta \neq 0$. The Gaussian curvature of the DNA ribbon, on the other hand, remains the same as for the ideal helicoid. The bending energy of the DNA ribbon can be calculated numerically by integrating the bending energy density over the midplane surface

$$U_{\text{DNA}} = \frac{\kappa}{2} \int_0^{z_m} dz \int_{-W/2}^{W/2} (H^2 - 2K) \sqrt{g} du . \quad (\text{S66})$$